An Efficient and High-Speed Disturbance Detection Algorithm Design with Emphasis on Operation of Static Transfer Switch

Adil USMAN[1], Mohammad Ahmad CHOUDHRY[2]
[1]*University of Engineering and Technology Taxila, Electronics Engineering Department, Pakistan*
[2]*University of Engineering and Technology Taxila, Electrical Engineering Department, Pakistan*
adil.usman@uettaxila.edu.pk

***Abstract*—Static Transfer Switch (STS) is required for high-speed transfer of essential load to the alternate power source when the main source fails due to power disturbance (PD). A fast and accurate PD detection method is required to ensure transfer time recommended by Computer Business Equipment Manufacturers Association (CBEMA) and IEEE Std. 446. This study encompasses the machine learning technique to reduce detection time for the disturbance on the preferred source. The 10 sample frames of acquired voltage signal were first differentiated and then distinctive features, i.e., Mean Absolute Deviation (MAD) and Energy (E) were extracted from the resultant frames. The features were fed to the Linear Support Vector Machine (L-SVM) classifier to detect the occurrence of PD events. The proposed approach achieved 100% accuracy for PD detection and detection time was significantly reduced. The system is robust in terms of unbalanced and marginal PDs. The system was validated using both simulated and real voltage signals. The proposed algorithm is easy to implement on an embedded system. Hence, detection time according to STS requirements can be achieved under various power system conditions.**

***Index Terms*—power quality, power system, event detection, feature extraction, support vector machine.**

I. INTRODUCTION

From the last few decades, innovations in the field of IT and power electronics has triggered the use of sensitive loads in the electric utility system. The industrial and commercial workplace is crowded with computer-based systems, digital signal processor-based medical equipment, lifesaving control systems, data centers, variable speed drives, and automated equipment in process industries [1]. These loads are vulnerable to power disturbances (PDs) such as voltage sag, voltage swell, and zero voltage interruptions. A few reasons for the voltage sag are: high inrush current with the starting of large electrical machines, sudden variation in load, and switching operation in the grid. Voltage interruption may occur due to utility failure or short circuit in the power network. Disturbance of even a few cycles is of great concern for the sensitive load. To avoid disruption in operation or severe damage to the equipment, the load has to be transferred to an alternate source. A conventional mechanical transfer switch (MTS) has a transfer time higher than two power cycles that may cause a momentary interruption of power. As a result, computer-based systems and other sensitive equipment can be damaged. The process industry may face substantial financial loss due to the malfunctioning of the programmable logic controllers (PLC).

A static transfer switch (STS) has been proposed in recent research for the fast transfer of electrical load [2-6]. Fig. 1 shows the fundamental building blocks of a three-phase STS. It includes a preferred source, alternate source, PD detection block, thyristor block, and load. When a disturbance occurs in the preferred source, the STS transfers the load from the preferred source to an alternate source [7]. The total transfer time (t_{tot}) of a transfer switch is a sum of detection time ($t_{\det}$) of disturbance in preferred source and time (t_{tr}) to transfer load from the preferred source to alternate source. Detection of disturbance and load transfer from the preferred power source to an alternative power source within safe time bounds is very critical. These time bounds are suggested by the Computer Business Equipment Manufacturers Association (CBEMA) and IEEE Std. 446 [8-9]. According to these standards, a decrease in a nominal voltage by 30% for more than 1/2 cycle time and zero voltage disturbance for more than 1/4 cycle time would cause malfunctioning in the sensitive equipment. Therefore, the load must be transferred to the alternate source within these time limits.

$$t_{tot} = t_{\det} + t_{tr} \tag{1}$$

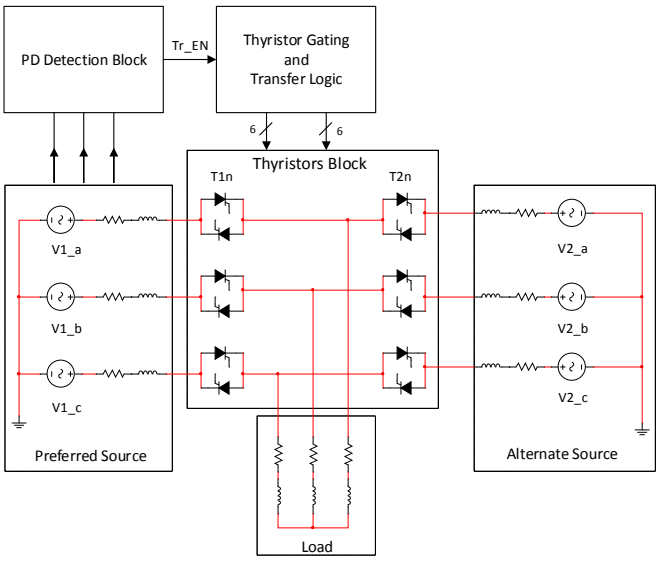

Figure 1. Placement and functioning of power disturbance detection block in the Static Transfer Switch System

Digital Object Identifier 10.4316/AECE.2021.02010

II. An Overview of Disturbance Detection Techniques

In recent studies, there are two types of techniques that have been used for disturbance detection in the power source. The first type is abc-to-dq0 transformation and the second one involves machine learning schemes based on feature extraction and classification. The abc-to-dq0 transformation based detection method has been used in the thyristor-based STS model [9]. Line voltages are transformed into a synchronously rotating frame, and this change of variables is done through Park's transformation matrix. The transfer time in these simulation-based STS models is summarized in the range of 4.1ms to 7.91ms under different conditions. The sampling frequency was 6.66kHz. This technique was also used in a benchmark system for the simulation of a thyristor-based STS. The detection time was achieved in the range of 0.46ms to 4.65ms under various loading conditions. It is worth mentioning that the abc-dq0 transformation based detection is the most commonly used PD detection method for transfer decisions in most of the STS models. Many researchers used abc-dq0 transformation method for the performance evaluation of these STS models [10-16]. Although the performance of abc-dq0 method is appreciable in the case of balanced disturbance events with significant deviations the inaccuracy is very high for unbalance disturbances and against all types of faint events. The hybrid event consisting of low magnitude disturbance (20% or lower) and significant unbalance of source voltage in more than one phase may remain undetected. STS fails to transfer the load from the preferred source to an alternate source due to these undetected hybrid events. Such events with substantial unbalance can severely damage the critical load if it remains connected to the preferred source. Moreover, the marginal variations in source voltages may lead to unwanted detections even when these variations are within acceptable limits. Most importantly, there are many events for which the processing time of this detection algorithm is more than 5ms [17]. Whereas, the total time of transferring the load from the preferred source to an alternate source, including detection time, must be less than 5ms for 50Hz power frequency.

A windowing-based voltage sag detection method for a hybrid automatic transfer switch (HATS) has been found in the literature. In this method, the difference between the current value and the value of a cycle before was calculated. Similarly, the current derivative value and that of a cycle before were calculated. The accuracy of the proposed method is claimed to be very high as there is no dead zone of detection, but there is no clue about its detection time. However, it is expected to take more than one cycle to detect the disturbance. Moreover, the accuracy of detection is compromised when a decrease of voltage is slow [18]. The PD detection using a 90-degree sliding window (quadrature) method was performed by researchers. The simulation and LabVIEW-based experimental results showed encouraging results with respect to detection time [19]. The disturbance events detection algorithm using a hybrid of the abc-dq0 transformation and 90^0 phase shift algorithm reduced the detection time to less than 0.25 of a cycle [20]. This method is not feasible for the STS application because this much time should be the total transfer time rather than detection time.

Several feature extraction and classification-based PD detection methods have been proposed, which can also be considered for the STS operations. In the first step, the dominant features are taken out of the source voltage signals. In the second step, the PD's are detected using classifier algorithms based on these features. A sag/swell detection algorithm based on wavelet transform (WT) operating in the presence of flicker and harmonics in source voltage was given. This algorithm is the hybrid of Daubechies wavelets of order 2 (db2) and order 8 (db8) to detect voltage sag/swell with and without positive/negative phase jumps. The performance of this method with respect to accuracy and detection time is better than Fast Fourier Transform (FFT) and Enhanced Phase Locked Loop (EPLL) based voltage sag/swell detection methods. The detection times of the start and end of voltage sag/swell with and without phase jump were claimed within 0.5ms and 1.15ms, respectively [21]. A disturbance detection method using WT was presented and less than ¼ cycle detection time was shown [22]. A combination of a histogram and discrete wavelet transform (DWT) methods for feature extraction and extreme learning machine (ELM) classification method resulted in 100% accuracy and 8.2s processing time [23]. Discrete wavelet transform, mathematical morphology, Singular Value Decomposition (SVD), and statistical analysis implemented on FPGA-based circuit for disturbance recognition showed remarkable results. The accuracy of around 100% and the processing time of 4679ms were claimed on simulation [24]. The DWT-based disturbance detection methods exhibit very high accuracy but due to the large number of features involved, they may not guarantee the time limit of the transfer signal generation while implementing real systems.

The hybrid of variational mode decomposition (VMD) and S-transform (ST) as feature extraction and SVM as a classifier has an overall accuracy of 99.66% [1]. Double-resolution S-transform (DRST) and directed acyclic graph support vector machines (DAG-SVMs) simulated and implemented on the DSP kit showed good accuracy of detection with a minimum computation time of 7.5ms [25]. Kullback–Leibler Divergence (KLD) and Standard deviation used with Support Vector Machine (SVM) to detect disturbance events have an accuracy of 94.02% [26]. In a detection scheme, a combination of flexible entropy-based feature selection (FEFS) and multi-class SVM (MC-SVM) was proposed. The maximum detection accuracy of 98.65% and minimum processing time around 140ms were claimed [27]. Multiresolution S-transform (MST) and decision tree (DT) based recognition method offered greater than 99% accuracy with a minimum detection time of 900ms [28]. An automated recognition approach for the classification of power disturbances based on empirical wavelet transform (EWT) as a feature extraction method and a multiclass support vector machine (SVM) as a classifier has been reported [29]. In a detection scheme, a microcontroller was used for the acquisition of source signal data and then fed to MATLAB in PC. A fusion of time-domain descriptors (TDD) at the feature extraction stage, multiclass support vector machine, and Naïves Bayes (NB) at the classification

stage was implemented. The accuracy of this method with both the classifier i.e. TDD+SVM & TDD+NB was shown more than 95.11% [30]. Wavelet Transforms (WT) and Support Vector Machines (SVM) based PD classifier with the low computational cost were proposed by De Yong, and accuracy was claimed 93.43% for a single event, 92.65% for two events in one simulated waveform [31]. The techniques presented in the literature which incorporate the SVM in the classification stage cannot ensure the accurate decision of load transfer if the above-mentioned feature extraction techniques are used. Therefore, SVM with these feature extraction techniques cannot be implemented in the STS control block.

Some neural network-based PD detection techniques have also been reported in the literature. A combination algorithm of empirical mode decomposition (EMD), the moments of a random variable, and an artificial neural network (ANN) have a computation time of 210ms. The accuracy of 100% was shown on synthetic and real signals [32]. An average accuracy of disturbance detection using Hilbert–Huang Transform (HHT) and Probabilistic Neural Network (PNN) was 91.6% [33]. The combination of the Stockwell Transform (SWT) feature extraction technique and neural network (NN) classifier showed an average accuracy of 94.7% and a detection time of 41ms [34]. A microcontroller-based real-time disturbance monitoring device was developed using DWT and ANN which demonstrated 100% accuracy with 200ms processing time [35]. This can be observed that the processing time of neural network-based disturbance detection algorithms is too long due to the high computational cost [36]. Therefore, the neural network cannot fulfill the STS requirements.

The voltage sag detection based on a single-phase rotating frame (SPRF) offers detection time in a range of 1ms to 8.8ms [37]. Detection and classification of PD events were performed using Sparse Signal Decomposition (SSD) and attained average accuracy of 97.11% [38]. The study based on the time-domain symmetrical components (TDSC) method reported an average lapse time of 31ms and a MATLAB function was incorporated for the demonstration of this detection time [39]. The detection of disturbance in power source using deep learning based on stacked autoencoder (SA) offers an average accuracy of detection around 99% [40]. The Independent Component Analysis (ICA) technique of sag/swell detection proposed in a previous study showed better accuracy as compared to the wavelet transform (WT) [41]. According to the harmonic footprints (HF) based detection method the voltage dip can be detected in less than 1ms but with an average accuracy of 97% [42]. The recursive technique for voltage dips detection like extended Kalman filtering does not present good results with respect to detection time [43]. An FPGA-based monitoring system for source voltage fluctuation using higher-order statistics (HoS) and Neuro Tree (NT) presented around 97% accuracy. The average detection time of 3-band WPT is 3.055s which is less than that of WPT but it is still a very long processing time [44]. The modified S-transform (MST) with parallel stacked sparse autoencoder (PSSAE) disturbance detection technique exhibited accuracy of 99.06% but with an average test time of 8.7ms [45]. In a recent study, it was shown that Improved Ensemble Empirical Mode Decomposition (IEEMD) takes 6s to detect the power disturbance which is a very long processing time. Moreover, the Empirical Mode Decomposition (EMD) and WT-based detection scheme was also compared with IEEMD based method. The results of this study revealed that the running time of the compared method is less than a proposed algorithm. Importantly, the algorithm was tested on noiseless disturbance signals only. Therefore, its performance and effectiveness cannot be predicted with respect to implementation on a real system [46]. Table I gives an overview of the disturbance detection methods for their accuracy and processing time.

TABLE I. AN OVERVIEW OF POWER DISTURBANCE DETECTION METHODS FOR THEIR ACCURACY AND PROCESSING TIME

Method	Database	Accuracy%	Processing time (ms)	Sampling Frequency (kHz)
SPRF	Synthetic and Real	-	1 - 8.8	120 3
abc-dq0 and 90^0 phase- shift algorithm	Synthetic	-	< 0.25 cycle	-
EMD, ANN	Synthetic and Real	100	210	20.48
abc-to-dq0	Synthetic and Real	-	≈ 5	6.6
TDSC	Synthetic and Real	-	31	6.6
DRST, DAG-SVM	Synthetic and Real	80	7.5	5
WT	Synthetic	-	< 0.25 cycle	-
SWT, NN	Synthetic	94.7	41	10
HF	Synthetic and Real	97	< 1	7.68 4.8
Kalman Filtering	Synthetic	-	3 - 10.47	-
DWT and ANN	Real	100	200	6.4
FEFS, MC-SVM	Synthetic	98.65	140	-
DWT, SVD	Synthetic and Real	100	4679 2.99	20.48
M-WPT WPT	Synthetic	-	3055 4056.25	-
MST, PSSAE	Synthetic and Real	99.06	8.7	5
MST, DT	Synthetic	99	900	3.2
FTDD, M-SVM, NB	Real	>99	7820	-
IEEMD	Synthetic	-	6000	-

The PD detection methods based on feature extraction and classification reported in the literature generally involve complex computation [47-49]. The total detection time comprises feature extraction time, and the classifier elapsed time. Usually, these methods use multiple features to attain the accuracy of detection, which increases the feature extraction time. The classification methods are also not computationally efficient because classification algorithms consume plenty of time in processing. The detection time becomes more vulnerable when more than one classifier is used in the classification step. The machine learning detection schemes do not present the accuracy and the detection time according to the STS requirements at the same time. However, the study of machine learning methods gives a pathway to reduce the computational cost and hence the processing time using optimal feature selection [48-49].

These studies showed that the higher the number of features used for detection or classification higher is the computation time. Moreover, lower the sampling rate of generated data lowers the computation time. Hence by selecting optimum features and sampling frequency the PD detection time can be reduced. So, if the machine learning technique has to be adopted for the disturbance detection in the STS application then a minimum number of those significant features that involve less computation and computationally efficient classifier will have to be selected.

The literature related to STS suggests that in order to avoid momentary disconnection, the time margin available for the transfer of load to an alternate source is less than ¼ cycle. So, screening must be accomplished within 2.5ms approximately to accommodate the inherent switching time of thyristors of both sources. It is noteworthy that the required total transfer time (t_{tot}) could not be ensured by STS and hence, could not be implemented practically yet. This is because under varying load and unbalanced disturbance situations, the accuracy of detection is compromised, and it may take greater than ¼ cycle to detect the disturbance resulting in a long transfer time. As a result, the efficiency of STS decreases if the detection algorithm fails to detect the deviations accurately within the required time limits. Therefore, to design an efficient and reliable STS, there is a need for accurate detection of PD in the preferred source in the minimum possible time.

III. Key Contributions

The major contributions of the proposed method can be listed as:

- The proposed system achieved 100% detection accuracy on three of the most relevant disturbances i.e., sag, swell, and interruption for STS.
- The parallel processing of the presented method shows accurate results against all types of unbalanced disturbances.
- The proposed detection method was evaluated on synthetic as well as real PD signal data
- The presented detection scheme has reduced detection time resulting decrease in total transfer time of STS.
- The proposed algorithm is feasible to implement on an embedded system for detection module in the control block of STS.

The rest of the article is arranged as follows: the conceptual framework of the proposed disturbance detection methodology is given in section IV in which all the individual blocks of the proposed scheme including, signal data acquisition, framing and differentiation, feature extraction, and detection using SVM classifier are explained.

The results of different experiments on synthetic and real PD signals are arranged in section V. The discussion and comparison of the proposed algorithm with different detection methods are covered in section VI. Finally, the article is concluded in section VII.

IV. Conceptual Framework for Proposed Disturbance Detection Methodology

A. System Overview

Fig. 2 presents the block diagram of the proposed disturbance detection scheme. It comprises five main processing stages: acquisition of voltage signals, framing, differentiation, feature extraction, and classification. First of all, the PD signal is acquired from a three-phase power source. In this work, two sets of voltage source signals were used to validate the proposed approach for PD detection: a collection of signals synthetically generated in computer simulation and a set of experimentally obtained real signals. In the second step, the framing of the acquired signal is performed which results from 10-sample frames of the input signal. Then derivative of each 10-sample frame is calculated. MAD and E features are then extracted from the resultant frame. After that, these features are fed to the SVM classifier with the linear kernel to detect disturbance. An identical detection scheme is applied on each phase of the three-phase power source independently for each phase in a parallel manner. The detection result of each phase in the form of a binary decision signal is fed to the OR gate. The output of this logical operation is the transfer enable signal. So, it makes the proposed detection scheme able to detect any type of disturbance in any phase of the three-phase power source at any time instant. The transfer enable signal generated by the OR gate will be used to initiate the transfer process in the control block of the STS.

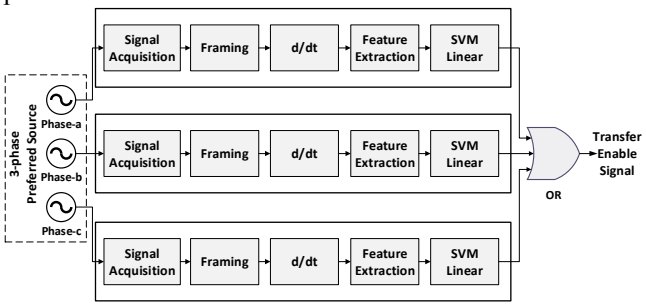

Figure 2. Block diagram of the proposed PD detection method for 3-phase power source

B. PD Signal Data Acquisition

The evaluation of the proposed algorithm was performed in a computer simulation using artificially generated and real signal data. Since the interruption, voltage sag, and voltage swell are the most relevant disturbances to the sensitive loads, therefore, the proposed algorithm in this paper was trained and tested on these three disturbances. Thus, a total of 3000 simulated signals with 1000 signals of each mentioned type were produced by varying the magnitude and time of random occurrence of disturbance. To balance the dataset, an equal number of normal source voltage signals were also generated. To show the effectiveness of the proposed method, it was also tested on real signal data set, having 1000 signals of each normal, interruption, sag, and swell. Table II shows the details of the acquired dataset.

Table III gives the simulation-based PD models of normal source voltage, interruption, sag, and swell as per the definition of international standards for monitoring electric PQ. Ten-cycle voltage data of each pure sine wave signal, interruption, sag, and swell were generated. It is observed

that PD signals generated with high sampling frequency in simulation increase the number of samples per cycle. Consequently, it increases the resolution of the signal and as a result, the computational cost is increased. On contrary, if we use a low sampling rate then a few samples give a deprived resolution of the signal which may lose the required information. The sampling frequency of data generation was 10kHz resulting in 2000 points in a 200ms period. The fundamental frequency of each signal was 50Hz. The simulated signals are shown in Fig. 3.

TABLE II. PD SIGNALS DATASET ACQUIRED USING COMPUTER SIMULATION AND HARDWARE SETUP

Type	PD Type	Simulated	Real	Total
Normal	Pure Sine	3000	1000	4000
Disturbance	Interruption	1000	1000	2000
	Sag	1000	1000	2000
	Swell	1000	1000	2000
	Total			**10000**

TABLE III. MATHEMATICAL MODELS OF DIFFERENT PD SIGNALS

Type	Signal	Mathematical Model	Parameters
Normal	Pure Sine wave	$v(t) = A \times \sin(\omega t)$	$\omega = 2\pi \times 50$ rad/sec
Disturbance	Interruption	$v(t) = A(1 - \rho(u(t-t_1) - u(t-t_2))) \times \sin(\omega t)$	$0.9 \le \rho \le 1$, $T \le t_2 - t_1 \le 9T$
	Sag	$v(t) = A(1 - \rho(u(t-t_1) - u(t-t_2))) \times \sin(\omega t)$	$0.1 \le \rho \le 0.9$, $T \le t_2 - t_1 \le 9T$
	Swell	$v(t) = A(1 + \rho(u(t-t_1) - u(t-t_2))) \times \sin(\omega t)$	$0.1 \le \rho \le 0.8$, $T \le t_2 - t_1 \le 9T$

In Table III, 'A' and 'ω' are the amplitude and angular frequency of the signal, respectively, and '$u(t)$' is the step function. 'ρ' is the signal component amplitude which is used to introduce voltage disturbance in the signal. All treated signals were defined in per-unit (p.u) so that the proposed methodology can be applied to any voltage range.

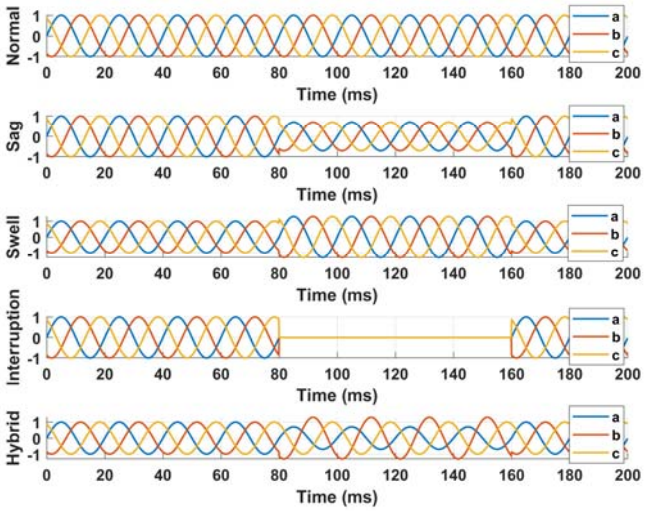

Figure 3. Waveforms of generated normal, interruption, sag, swell and hybrid events

To show the efficiency of the proposed method for PD detection, it is necessary to consider real signals as well. Fig. 4 shows the experimental setup for the three-phase source voltage signal acquisition. The data acquisition system (DAS) consisted of three identical circuits based on the potential transformer (PT) ZMPT101b for each phase, MyDAQ from National Instruments (NI), and NI LabView software. A voltage signal of each phase was acquired through PT, conditioned by a circuit, and digitizing with MyDAQ. That was connected to a PC via USB port, and the data were recorded using LabVIEW. DAS acquired 4000 signals at a sampling rate of 10 kHz.

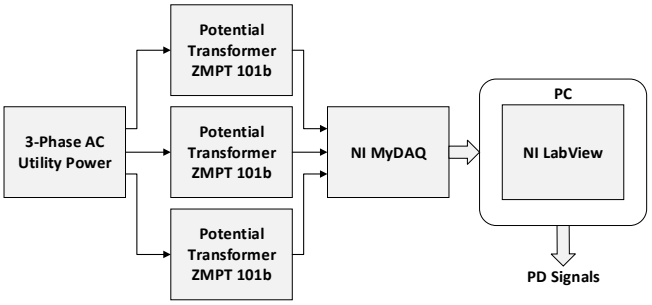

Figure 4. Block diagram of hardware setup used for real PD signal acquisition

C. *Framing and Differentiation*

After voltage signal acquisition, all the remaining steps with experimentation were simulated in MATLAB. Differentiation was performed on a sliding window with 10-samples in length. This window size was selected to reduce computational complexity and hence the detection time which is the key requirement of STS for fast load transfer. The time of analysis and computation can be reduced with a smaller window size provided the rate of the correct decision remains adequate. So, our algorithm has to analyze and process only 10 data points in the current frame and making a decision about the occurrence of disturbance. A derivative of a function itself represents a change in the function values. The derivative values of a signal would be more observable if the change is sudden and the rate of change is high. Since the alternating voltage signal is itself changing with respect to time, therefore, using the derivative of disturbance signal directly to detect the PD event would not help in case of sag, swell, and normal due to similarity in signal shape. But features of the derivative signal instead of raw signal signify the change in PD signal when any disturbance event occurs. Therefore, the distinguishing features which involve minimal computations were extracted from the differentiated frame.

D. *Feature Extraction*

In this work, extensive experimentation was performed to find out the significant features that can exhibit the best results to fulfill the STS requirements in the detection phase. So, fifteen discriminated computationally simple features were extracted from the differentiated signal of the preferred voltage source as defined in Table IV. Moreover, most of these features have shown good results with respect to accuracy in the literature related to power disturbance detection and classification [50-52]. The definition of these features indicates that their values will show significant change when a disruption occurs in the input PD signal. The mean (M) is the average value of a signal. An AC signal fluctuates around its mean value. If the signal is a periodic waveform, like a sine wave, it can be quantified by its peak-to-peak amplitude. Unfortunately, the disturbance signals are random in nature and do not show a well-defined peak-to-peak value. The standard deviation (SD) is a measure of

how far the signal deviates from the mean. Skewness (Skw) is the measure of distortion from the normal distribution and measures the lack of symmetry in the data distribution. The perfect sine-wave should have skewness equal to zero but any deviation can result in positive or negative skewness which may be helpful in this problem. Kurtosis (KUR) is actually the measure of outliers present in the data distribution. The disturbance signal will definitely have outliers in the data points which can be quantified by KUR. The root mean square (RMS) and peak-to-peak (pk_pk) have been commonly used in power disturbance detection due to directly observable changes in their values. The crest factor (CF) is the comparison of a peak value of the signal to its RMS value, Shape factor (SF) is the ratio of RMS value and absolute mean value, impulse factor (IF) is the ratio of peak value to its absolute mean value and the margin factor (MF) is the ratio of peak value to its square of the absolute mean value. Energy (E) is the measure of the quantitative strength of a signal which implicitly helpful in detecting the change in normal signal. Similarly, the log energy (LogE) and Shannon energy (SE) can also be employed to find out the observable change in the input voltage.

TABLE IV. DESCRIPTION OF SIGNIFICANT FEATURES EXTRACTED FROM THE DIFFERENTIATED FRAME X

Feature	Formula
Mean (M)	$M = \frac{1}{n}\sum_{i=1}^{n}(X_i)$
Standard Deviation (SD)	$\delta = \sqrt{\frac{\sum_{i=1}^{n}(X_i - X_{avg})^2}{n}}$
Skewness (Skw)	$Skw = \frac{1}{n}\frac{\sum_{i=1}^{n}(X_i - X_{avg})^3}{\delta^3}$
Kurtosis (KUR)	$KUR = \frac{1}{n}\frac{\sum_{i=1}^{n}(X_i - X_{avg})^4}{\delta^4}$
Root Mean Square (RMS)	$RMS = \sqrt{\frac{1}{n}\sum_{i=1}^{n}(X_i)^2}$
Crest Factor (CF)	$CF = \frac{X_{peak}}{RMS}$
Shape Factor (SF)	$SF = \frac{RMS}{X_{am}}$
***Impulse Factor (IF)**	$IF = \frac{X_{peak}}{X_{am}}$
Margin Factor (MF)	$MF = \frac{X_{peak}}{X_{am}^{\ 2}}$
Energy (E)	$E = \sum_{i=1}^{n}(X_i)^2$
Log Energy (LogE)	$LE = \sum_{i=1}^{n}\log(X_i^{\ 2})$
Shannon Energy (SE)	$SE = -\sum_{i-1}^{n}X_i^{\ 2}\log(X_i^{\ 2})$
Mean Absolute Deviation (MAD)	$MAD = \frac{1}{n}\sum_{i=1}^{n}(\lvert X_i - M\rvert)$
***Median Absolute Deviation (MedAD)**	$MeAD = \frac{1}{n}\sum_{i=1}^{n}(\lvert X_i - Med\rvert)$

* X_{peak} is the peak value, X_{am} is the absolute mean, Med is the median of X

The mean absolute deviation (MAD) of a signal is the average distance between each data point and the mean. It gives us an idea about the variability in a dataset. The median absolute deviation (MedAD) also gives the measure of the unevenness of data points.

Table V gives the statistics of these features, which depicts the significance of these features because the mean and standard deviation of these features of disturbance input voltage signal is meaningfully different from the normal one.

TABLE V. STATISTICAL PARAMETERS ILLUSTRATING THE SIGNIFICANT DIFFERENCE IN AASE OF NORMAL AND DISTURBANCE SIGNAL

Features/Classes	Disturbance		Normal	
	M	**SD**	**M**	**SD**
M	0.000987	0.0552695	-0.0020214	0.0441445
SD	0.293166	0.206126	0.0034547	0.0016438
Skw	0.0212628	1.3074016	0.0062065	0.3112048
KUR	5.118042	1.0006472	1.8534505	0.2320191
Pk_Pk	1.1290107	0.8326008	0.0100712	0.0048123
RMS	0.2864634	0.1875034	0.0400997	0.0189029
CF	1.814941	0.8487631	0.2251503	1.0219414
SF	1.7636009	0.4094346	1.0309902	0.0602481
IF	3.277633	1.8122116	0.2531591	1.065699
MF	24.8804	20.643553	32.805323	97.173799
E	1.0549342	1.2592481	0.0176867	0.0124436
LogE	0.770319	1.423488	4.6031732	1.401803
SE	0.0123444	1.1813067	0.1046813	0.0677169
MAD	0.1437501	0.0941881	0.0028133	0.0013345
MedAD	0.0073186	0.0102632	0.0025827	0.0012044

E. Detection using Support Vector Machine

After the feature extraction from differentiated three-phase voltage source signals, the disturbance detection was accomplished using a machine learning algorithm. In this study, the support vector machine (SVM) was proposed due to its high accuracy of classification [53-57]. A linear kernel was used because of its low computational cost. Generally, the objective of L-SVM is to separate two categories and hence suitable for distinguishing between the disturbance and normal signal. SVM is a supervised learning technique that builds an optimal separating hyperplane by maximizing the margin between the hyperplane and dataset. It is used for the detection of any deviance from a particular class of data.

It is supposed that, $v_i \in R^m$ is the input feature vector obtained from differentiated frame X and $g_i \in \{+1, -1\}$ denotes two classes i.e. disturbance and normal, the group of data is $S = \{v_i, g_i\}_{i=1}^{n}$, and where n is the sample number. Consider $f(v) = 0$ is the hyperplane separating the input data, which is linearly separable.

$$f(v) = w.v + b = \sum_{j=1}^{n} w_j \times v_j + b = 0 \quad (1)$$

where, w and b represent the weight and bias, respectively. They optimize the position of the separating hyperplane satisfying the following restriction:

$$g_i f(v_i) = g_i(w.v_i + b) \geq 1, \quad i = 1, 2, ...n \quad (2)$$

If variable d_i denotes the distance between the margin and the input vector v_i which is on the false side of the margin then the following optimization problem will result in the optimized separating hyperplane:

$$\text{Minimize} \quad \tfrac{1}{2} \times \|w\|^2 + e\sum_{i=1}^{n} d_i, \quad i = 1, 2, ...n$$

$$\text{Subject to} \quad \left\{ \begin{matrix} g_i(w.v+b) \geq 1-d_i \\ d_i \geq 0 \end{matrix} \right\}$$

where, e is error compensation.

The above problem can be formulated as follows:

$$\text{Maximize} \quad \sum_{i=1}^{n} \alpha_i - \tfrac{1}{2} \times \sum_{k=1}^{n} \alpha_i \alpha_k y_i y_k K(v_i, v_k)$$

$$\text{Subject to} \quad \sum_{i=1}^{n} \alpha_i g_i = 0, \quad \alpha_i \geq 0, \quad i = 1, 2, ...n$$

where, α_i is a Lagrange multiplier and $K(v_i, v_k) = v_i^T v_k$ is the linear kernel function .

Finally, a separating hyperplane will be constructed between feature points of disturbance and normal signals at optimized positions resulting in detection of disturbance. The MATLAB classification learner application was used to train the proposed model. The parameters of the trained model were used to test the algorithm.

V. RESULTS

A. Experimental setup

To achieve a fast transfer of load from preferred source to alternate source, an accurate power disturbance detection system has to be designed that has minimum processing time. The implementation of the proposed method involved two stages presented in Fig. 5. The first one was the training of L-SVM using all the steps involved in the proposed detection scheme presented in section 5. The classifier was trained using 6000 synthetically generated and 4000 experimentally obtained real PD signal datasets shown in Table II.

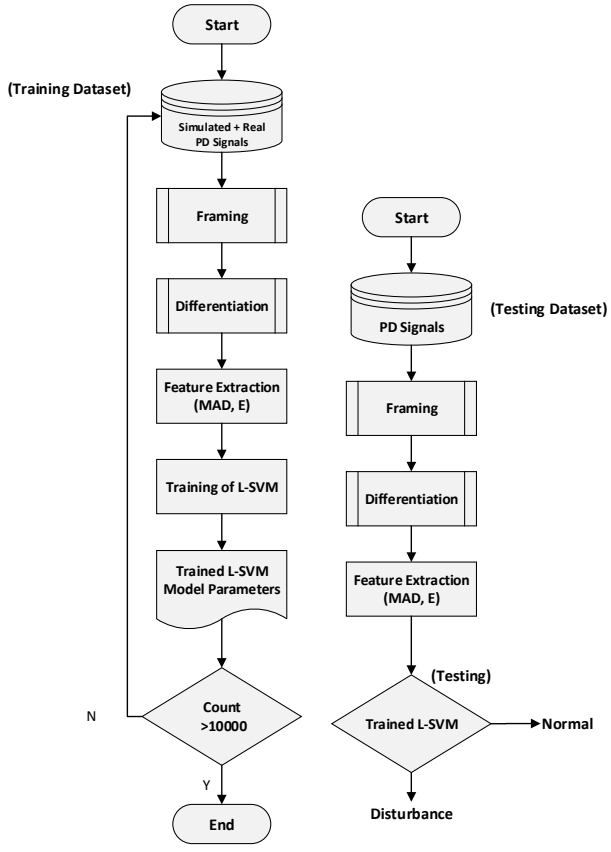

Figure 5. Flow charts of Training and Testing algorithms of the proposed detection method

The training was performed in MATLAB software and trained classifier model parameters were obtained. In the second stage, the validation of the algorithm against any PD signal was carried out. The platform for the testing algorithm can either be MATLAB software or an embedded controller. However, the former has been utilized in this paper for validation purposes. The real and simulated disturbance signals from the testing dataset were fed to the algorithm in a random sequence. The performance of SVM is measured through classification accuracy averaged over k-fold cross-validation. In order to attain the best accuracy with low bias, modest variance, and low correlation, the value of k = 10 has been selected based on experimentation. The testing dataset comprises 3 groups of disturbance signals:

1. 5000 simulated signals;
2. 2500 real signals;
3. 2500 noisy signals.

Each group contains 15% disturbance signals of each type i.e., 3-phase sag, 3-phase swell, 3-phase interruption and normal, 10% marginal disturbance signals with amplitude 0.91p.u. to 1.09p.u., 10% faint disturbance signals (with 20% or lower magnitude), 10% of signals having hybrid events, 10% of signals having disturbance events due to single-phase to ground fault and phase to phase fault. The processing/detection time of the testing algorithm is defined as the sum of framing, differentiation, features extraction, and classification of the current input signal.

B. Results with Synthetic PD Signals

Thorough and methodical experimentation was performed, and all the possible combinations of 15 features defined in Table IV were tested with different classifiers. The feature selection criteria of this experimentation are to test all the possible combinations of all these classifiers with the features stated above. Then combination is selected which may exhibit high accuracy with a minimum number of features and hence with minimum computation time. Table VI shows the maximum attainable accuracies of each classifier with combinations of fifteen features are presented which indicates that the L-SVM shows 100% accuracy with only two features i.e. MAD and E. So, this particular combination is expected to be computationally more efficient than other combinations. It can also be observed that features like Pk_Pk, CF, SF, IF, MF, LogE, and SE are nowhere in Table VI and hence do not contribute to defining the good accuracies. The extended version of Table VI is presented in Table A1 in appendix A.

TABLE VI. MAXIMUM ATTAINABLE ACCURACIES OF CLASSIFIERS WITH DIFFERENT FEATURE COMBINATIONS

M	SD	Skw	KUR	RMS	E	MAD	MedAD	# of Features	Accuracy
1	1	0	1	0	0	0	0	3	DTs: 99.99%
0	1	0	1	1	0	0	0	3	QDs: 100%
0	1	0	1	1	0	0	0	3	LR: 100%
0	1	0	0	1	0	1	1	4	KNB: 99.99%
0	1	0	0	1	0	1	0	3	F-KNN: 100%
0	0	1	1	1	0	1	0	4	EBT: 99.9%
0	0	0	0	0	1	1	0	2	L-SVM: 100%

Fig. 6 shows the confusion matrix of the decision of the proposed detection system between the normal and disturbance in the source. To obtain the confusion matrix, the accuracy is measured according to the following formula.

$$Accuracy = \frac{TP + TN}{TP + TN + FP + FN} \quad (3)$$

where, *TP* stands for true positive, *TN* for true negative, *FP* for false positive, and *FN* for false negative. By substituting the obtained *TP*s, *TN*s, *FP*s, and *FN*s from the confusion matrix in Equation (3), the Overall Average Accuracy achieved is 100%. L-SVM with MAD and E features correctly detected 1500 signals of normal sine wave out of a total of 1500. The erroneously predicted samples are zero i.e. *FN*. In the same way, out of 1500 power disturbance signals, L-SVM correctly predicted 1500 signals which is *TN* and none of them was incorrectly predicted. The total classification accuracy of L-SVM is found to be 100% according to the above parameters.

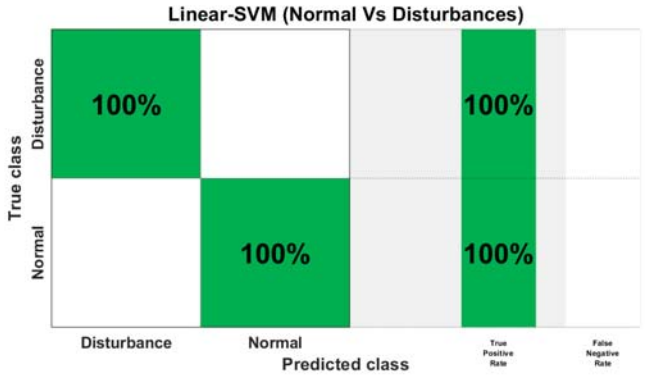

Figure 6. Confusion matrix of the proposed detection method

The Receiver operating characteristic (ROC) curve is generally plotted to evaluate the performance of detection algorithms [63]. Fig. 7 shows the ROC curve of L-SVM for this investigation. The curve is a plot between the true positive rate and the false positive rate. The Area under the ROC curve (AUC) gives us the classifier performance. The AUC measured for the L-SVM classifier is 1, which endorse the claimed results.

The PD detection time of each combination with maximum accuracies was computed and is highlighted in Table VII. The total detection time of the algorithm is equal to the sum of differentiation and feature extraction time, and classifier processing time. The experimental setup is composed of MATLAB2019a with a CPU (Intel Core i7-7700K, 3.6GHz, and 16G RAM). The combinations are labeled with the name of classifiers. Our investigation revealed that the combination of L-SVM with MAD and E features demonstrates 100% accuracy and the lowest mean detection time of 5.938ms. Moreover, the algorithm can detect the power disturbance using just 10 data points in one frame of the input voltage signal. The differentiation plus feature extraction time was found to be 2.321ms while the mean computation time of the L-SVM classifier was 3.617ms. If the detection algorithm developed on the MATLAB platform is implemented on an embedded controller using C++ or any low-level programming language, then the detection time is expected to be reduced to less than 2.5ms [58-60]. Moreover, many researchers have implemented machine learning algorithms in the field programmable gate array (FPGA). It was observed that the run-time was significantly reduced as compared to the elapsed time of the same algorithm when implemented on a

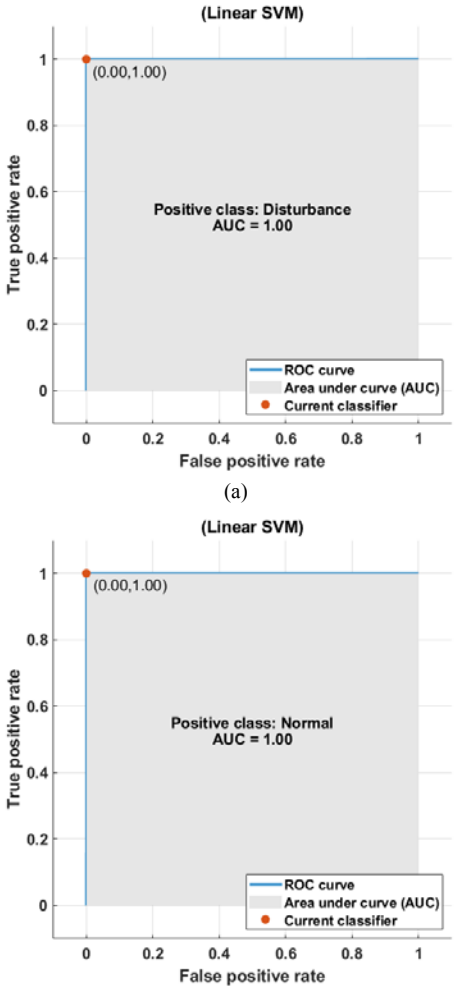

Figure 7. ROC curves of L-SVM classifier

software platform [61]. In addition to that, the algorithm has to process only one window of 10 samples which fulfills the requirement of STS and also making precise and accurate detection. Consequently, the use of this window size makes it feasible for the realization of the algorithm on an embedded system. It is worth mentioning that our proposal, using a sampling frequency of 10 kHz yielded results with a high ratio of success and adequate processing time making it possible to embed on a simple embedded controller.

TABLE VII. DETECTION TIMES OF COMBINATIONS WITH MAXIMUM ACCURACIES

Classifiers	Classification Time (s)	Differentiation and Feature Extraction Time (s)	Total Detection Time (s)
EBT	0.042623	0.010897	0.05352
F-KNN	0.004605	0.091029	0.095634
L-SVM	0.003617	0.002321	0.005938
KNB	0.009634	0.004699	0.014333
LR	0.006267	0.00442	0.010687
DT	0.004767	0.004996	0.009763
QD	0.004165	0.005294	0.009459

The accuracy of the detection system using the MAD and E features with different classifiers was also evaluated and is

presented in Fig. 8. It can be observed that L-SVM with selected features has outperformed the other combinations. Although some other classifiers also obtained high accuracies with these features, the processing time of L-SVM was the lowest.

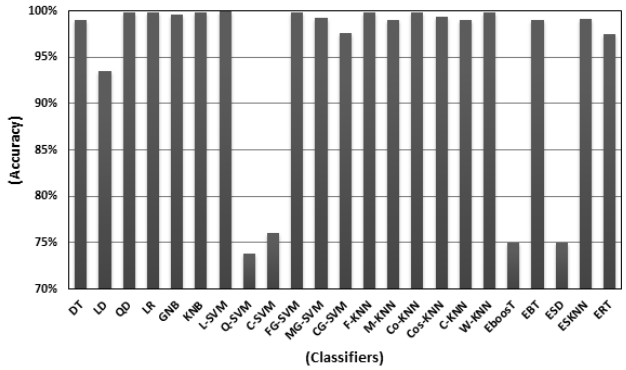

Figure 8. Accuracy of PD detection using MAD & E with different classifier

Usually, noise is superimposed on the voltage/current signals in a real electric power network. Noise in the electric power system can be caused by power electronic drives, control circuits, arcing apparatus, loads with solid-state rectifiers, and switching power supplies [62]. Therefore, the additive white Gaussian noise (AWGN) was added to PD signals with a signal-to-noise ratio (SNR) in the range of 10dB to 60dB, and a testing dataset of noisy disturbance signals was obtained. The effectiveness and sensitivity of the proposed method were evaluated under these noisy conditions. This gives an insight that how well this scheme would work if implemented on a real system. Fig. 9 shows the detection accuracy of the proposed method, which depicts that the proposed detection system offers robustness towards the noise.

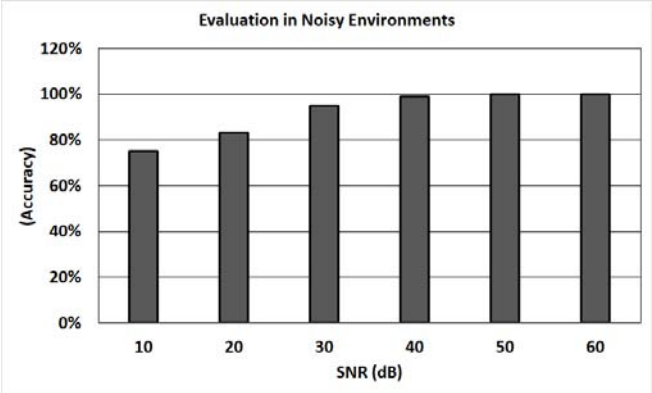

Figure 9. Percentage of correct detection results under different noisy conditions

C. Results with Real PD Signals

The detection block of the real STS system acquires voltage signal from utility using a voltage sensor and data acquisition device. So considering this real situation and to validate the performance, a testing dataset of real disturbance signals was acquired using hardware setup explained in section 5. The proposed PD detection method for STS was tested on real PD signals. These real signals were fed to the system, and the results obtained from this experiment verified the results obtained using the synthetic disturbance signals. Hence, the feasibility of the presented detection scheme was authenticated for STS.

VI. DISCUSSION

The proposed method of PD detection for the STS control module showed superior performance as compared to the abc-dq0 transformation method, which has been most consistently used by the researchers. The presented method has resolved the problem of the inaccurate decision of the abc-dq0 transformation based detection technique in case of unbalanced disturbances and faint events. As the proposed algorithm independently performs its processing on only one window of 10 samples of each phase, therefore, the accuracy and processing time remains unaffected in case of unbalanced phases. Moreover, the detection system was tested on the dataset containing disturbance signals with random amplitude and time of occurrence. The accuracy of 100% showed that the weak disturbances did not remain undetected. Also, the marginal variations within allowable limits (0.91p.u. to 1.09p.u.) were found to be undetected and hence avoiding unwanted transfer of load from preferred to an alternate source. The algorithm was applied to all the phases in a parallel fashion so that a significant unbalancing of source voltage in more than one phase might be detected successfully. So, hybrid disturbance events have not remained undetected using this scheme. Since the algorithm has been applied to each phase separately therefore it detected successfully the disturbances due to single-phase to ground fault and phase to phase fault. As the proposed method was trained on PD signals with high randomness in nature, therefore any significant disturbance at any time in any phase was detected with 100% accuracy. Extracting features from differentiated PD signal instead of from raw signal made this possible to reduce the number of features which reduced the computational cost of the detection algorithm. The overall mean processing time of the algorithm was found to be 5.938ms. Contrary to the windowing-based detection method, the presented algorithm can detect the disturbance signal without Fast Fourier Transform under the situation that voltage decreases gradually.

Table VIII shows the performance comparison of the proposed PD detection system with the other reported methods in terms of detection accuracy and detection time. The proposed approach outperformed the methods presented in the latest research. The detection time of the presented method in this study is lesser than the methods proposed by Sadigh, Kumar, Katic' and Kumawat. The computation time of the proposed algorithm is also better than a recently presented IEEMD based disturbance detection method. Although some methods also have 100% accuracy, their PD detection times were far greater than the proposed method. The reason behind the discrepancy in detection time is that these methods have to compute a large number of features resulting in dilation in feature extraction time. Also, these methods use classifiers with complex processing. Whereas the proposed algorithm needs only two features to be extracted and the L-SVM classifier presents very fast processing. The harmonic footprint method presented by researchers shows PD detection time, less than the available methods. However, its accuracy of detection is lower; so, it is not reliable for STS in transfer decision making. The sampling rate at which the synthetic signals were generated in this work is lesser than that of methods presented by

Sadigh and Lopez. So, it encourages us to believe that the algorithm can be implemented on a controller with a low sampling rate capability. Hence, the proposed detection scheme can be directly employed in the PD detection block of the controller for the STS system.

TABLE VIII. COMPARISON OF DETECTION/PROCESSING TIME OF PROPOSED METHOD WITH DETECTION SYSTEMS IN LITERATURE

Method	Mean Accuracy (%)	Detection time (ms)
SPRF [37]	-	1 - 8.8
EMD, ANN [32]	100	210
abc-to-dq0 [3-5,17]	-	≈ 5
TDSC [39]	-	31
DRST, DAG-SVM [25]	80	7.5
SWT, NN [34]	94.7	41
HF [42]	97	< 1
Kalman Filtering [43]	-	3 - 10.47
DWT, ANN [35]	100	200
FEFS, MC-SVM [27]	98.65	140
DWT, SVD [24]	100	4679 2.99
M-WPT WPT [44]	-	3055 4056.25
MST, PSSAE [45]	99.06	8.7
MST, DT [28]	99	900
FTDD, M-SVM, NB [30]	>99	7820
IEEMD [46]	-	6000
Proposed Method	**100**	**5.938**

VII. CONCLUSION

The PD detection methods used for static transfer switch (STS) were briefly reviewed, and the limitations were highlighted. In this research, the detection time (t_{det}) of disturbance in the voltage source was focused in order to reduce the total transfer time (t_{tot}) of the STS in line with the CBEMA curve. The proposed methodology was based on mean absolute deviation (MAD), and energy (E) features of derivative of one input frame, and detection using linear support vector machine (L-SVM) classifier. The process in this study showed superior performance than the abc-to-dq0 method, which is the most commonly employed PD detection method for STS. As the technique was applied to all the phases separately, the accuracy and detection time remained unaffected even in case of unbalanced events or any weak disturbance in the three-phase power supply. The low magnitude and hybrid events were also detected successfully. Moreover, the allowable marginal variations were rightly not identified to avoid the unnecessary transfer of load. Due to the least number of features and a linear basis of SVM, the proposed method was computationally efficient than PD detection methods presented in previous researches. The proposed technique detected a significant PD at any time of occurrence in any phase with remarkable accuracy and speed. Overall, the proposed method showed 100% accuracy of detection on three considered events and 5.938ms detection time, which has far better performance than the techniques presented in the literature. The major issues with previous detection methods have been resolved, and therefore the projected system can practically be implemented in the STS system. So, it can substantially reduce the total transfer time (t_{tot}) of STS when implemented on an embedded system. The major advantages of the proposed method are its reliability, precise operation, and easy implementation without using a phase lock loop (PLL). The practical aspects of the PD detection in the STS control block are entirely taken into account while implementing the proposed system in a computer simulation. This study proved good results in all considered real scenarios therefore, can be easily implemented in a real order. The window size equal to 10-samples, the use of only two simple features, the linear basis of SVM, and a sampling rate of 10kHz made this algorithm ready to be implemented on a real system. Hence, the detection time, less than 2.5ms, can be achieved by realizing this method on an embedded controller. A reliable and efficient STS can be developed using the proposed detection scheme.

The scope of the proposed detection system can be expanded to the equipment related to power system protection, instrumentation, and fault detection. In the future, we intend to work on a real-time disturbance monitoring system based on this method with required modifications. The proposed algorithm is tested on only three types of events and its performance on other power disturbances is untested. In the future, we have planned to evaluate the proposed methodology on different single events like harmonics, flicker, transients, notches, spikes, and combined events.

ABBREVIATIONS

The following abbreviations are used in this manuscript:

DT	Decision Trees
LD	Linear Discriminant
QD	Quadratic Discriminant
LR	Logistic Regression
GNB	Gaussian Naïve Bayes
KNB	Kernal Naïve Bayes
Q-SVM	SVM Quadratic
C-SVM	SVM Cubic
FG-SVM	Fine Gaussian SVM
MG-SVM	Medium Gaussian SVM
CG-SVM	Coarse Gaussian SVM
KNN	K-Nearest Neighbor
F-KNN	Fine KNN
M-KNN	Medium KNN
Co-KNN	Coarse KNN
Cos-KNN	Cosine KNN
C-KNN	Cubic KNN
W-KNN	Weighted KNN
EBoosT	Ensemble Boosted Trees
EBT	Ensemble Bagged Trees
ESD	Ensemble Subspace Discriminant
ESKNN	Ensemble Subspace KNN
ERT	Ensemble RUSBoosted Trees
CBEMA	Computer Business Equipment Manufacturers Association

APPENDIX A

TABLE A1. MAXIMUM ATTAINABLE ACCURACIES OF CLASSIFIERS WITH DIFFERENT FEATURE COMBINATIONS (EXTENDED VERSION TABLE VI)

M	1	0	0	0	0	0	0
SD	1	1	1	1	0	1	0
Skw	0	0	0	0	0	0	1
Kur	1	1	1	0	0	0	1
pk_pk	0	0	0	0	0	0	0
RMS	0	1	1	1	0	1	1
CF	0	0	0	0	0	0	0
SF	0	0	0	0	0	0	0
IF	0	0	0	0	0	0	0
MF	0	0	0	0	0	0	0
E	0	0	0	0	1	0	0

LogE	0	0	0	0	0	0	0
SF	0	0	0	0	0	0	0
MAD	0	0	0	1	1	1	1
MedAD	0	0	0	1	0	0	0
FT	99.90%	99.90%	99.90%	99.90%	99.90%	99.90%	99.90%
MT	99.90%	99.90%	99.90%	99.90%	99.90%	99.90%	99.90%
CT	99.90%	99.90%	99.90%	99.90%	99.90%	99.90%	99.90%
LD	98.50%	98.30%	98.30%	87.80%	93.60%	87.50%	98.50%
QD	99.40%	100%	100%	99.90%	99.90%	99.99%	99.30%
LR	99.80%	100%	100%	99.80%	99.90%	99.90%	99.99%
GNB	99.10%	99.30%	99.30%	99.80%	99.60%	99.80%	99.10%
KNB	99.80%	99.80%	99.80%	99.99%	99.90%	99.90%	99.80%
LSVM	99.80%	99.90%	99.90%	99.90%	100%	99.90%	99.80%
QSVM	99.90%	99.90%	99.90%	99.90%	66.40%	99.90%	99.90%
CSVM	99.90%	98.90%	98.90%	99.80%	58.80%	73.20%	100%
FGSVM	99.50%	99.80%	99.80%	99.90%	99.90%	99.90%	99.90%
MGSVM	99.30%	99.40%	99.40%	99.50%	99.30%	99.50%	99.50%
CGSVM	98.80%	99.00%	99.00%	97.50%	97.50%	98.00%	99.10%
FKNN	99.90%	99.90%	99.90%	99.90%	99.90%	100%	99.90%
MKNN	99.60%	99.80%	99.80%	99.90%	99.90%	99.90%	99.60%
CoarseKNN	99.00%	99.20%	99.20%	99.70%	99.90%	99.70%	99.10%
CosineKNN	99.50%	99.70%	99.70%	99.70%	99.40%	98.60%	99.60%
Cubic KNN	99.60%	99.80%	99.80%	99.90%	99.90%	99.90%	99.60%
WKNN	99.80%	99.90%	99.90%	99.90%	99.90%	99.90%	99.80%
EBoostT	75%	75%	75%	75%	75%	75%	75%
EBagT	99.90%	99.90%	99.90%	99.90%	99.90%	99.90%	99.90%
ESD	98.60%	98.50%	98.50%	93.80%	75%	89.10%	98.60%
ESKNN	99.70%	99.70%	99.70%	99.90%	99.2	99.90%	99.80%

REFERENCES

[1] A. A. Abdoos, P. K. Mianaei, and M. R. Ghadikolaei, "Combined VMD-SVM based feature selection method for classification of power quality events," Applied Soft Computing, vol. 38, pp. 637-646, Oct. 2016. doi:10.1016/j.asoc.2015.10.038

[2] H. Mokhtari, "High speed silicon controlled rectifier static transfer switch," National Library of Canada = Bibliothèque nationale du Canada, 2000

[3] H. Mokhtari, M. Iravani, S. Dewan, P. Lehn, and J. Martinez, "Benchmark systems for digital computer simulation of a static transfer switch," IEEE Power Engineering Review, vol. 21, pp. 69-69, Jul. 2001. doi:10.1109/MPER.2001.4311483

[4] M. Moschakis and N. Hatziargyriou, "A detailed model for a thyristor-based static transfer switch," IEEE Transactions on Power Delivery, vol. 18, pp. 1442-1449, Oct. 2003. doi:10.1109/TPWRD.2003.817790

[5] C. He, F. Li, and V. Sood, "Static transfer switch (STS) model in EMTPWorks RV," in Canadian Conference on Electrical and Computer Engineering 2004 (IEEE Cat. No. 04CH37513), 2004, Niagara Falls, pp. 111-116. doi:10.1109/CCECE.2004.1344969

[6] S.-M. Song, J.-Y. Kim, and I.-D. Kim, "New Three-Phase Static Transfer Switch using AC SSCB," in 2018 International Power Electronics Conference (IPEC-Niigata 2018-ECCE Asia), 2018, Niigata, pp. 3229-3236. doi:10.23919/IPEC.2018.8507620

[7] S. C. Yáñez-Campos, G. Cerda-Villafaña, and J. M. Lozano-Garcia, "Two-Feeder Dynamic Voltage Restorer for Application in Custom Power Parks," Energies, vol. 12, p. 3248, Aug. 2019. doi:10.3390/en12173248

[8] J. Schwartzenberg and R. De Doncker, "15 kV medium voltage static transfer switch," in IAS'95. Conference Record of the 1995 IEEE Industry Applications Conference Thirtieth IAS Annual Meeting, 1995, Orlando, pp. 2515-2520. doi:10.1109/IAS.1995.530623

[9] M. Faisal, M. A. Hannan, P. J. Ker, M. S. B. A. Rahman, M. S. Mollik, and M. B. Mansur, "Review of Solid State Transfer Switch on Requirements, Standards, Topologies, Control, and Switching Mechanisms: Issues and Challenges," Electronics, vol. 9, p. 1396, Aug. 2020. doi:10.3390/electronics9091396

[10] H. Mokhtari, S. B. Dewan, and M. Travani, "Performance evaluation of thyristor based static transfer switch," IEEE Transactions on Power Delivery, vol. 15, pp. 960-966, Jul. 2000. doi:10.1109/61.871359

[11] H. Mokhtari, S. B. Dewan, and M. R. Iravani, "Effect of regenerative load on a static transfer switch performance," IEEE transactions on power delivery, vol. 16, pp. 619-624, Oct. 2001. doi:10.1109/61.956747

[12] H. Mokhtari, "Performance evaluation of thyristor-based static transfer switch with respect to cross current," in IEEE/PES Transmission and Distribution Conference and Exhibition, 2002, Yokohama, pp. 1326-1331. doi:10.1109/TDC.2002.1177672

[13] H. Mokhtari, S. B. Dewan, and M. R. Iravani, "Analysis of a static transfer switch with respect to transfer time," IEEE Transactions on Power Delivery, vol. 17, pp. 190-199, Nov. 2001. doi:10.1109/MPER.2001.4311177

[14] A. Sannino, "Static transfer switch: analysis of switching conditions and actual transfer time," in 2001 IEEE Power Engineering Society Winter Meeting. Conference Proceedings (Cat. No. 01CH37194), 2001, Columbus, pp. 120-125. doi:10.1109/PESW.2001.917013

[15] H. Mokhtari and M. R. Iravani, "Effect of source phase difference on static transfer switch performance," IEEE transactions on power delivery, vol. 22, pp. 1125-1131, Apr. 2007. doi:10.1109/TPWRD.2006.883004

[16] H. Mokhtari and M. R. Iravani, "Impact of difference of feeder impedances on the performance of a static transfer switch," IEEE transactions on power delivery, vol. 19, pp. 679-685, Mar. 2004. doi:10.1109/TPWRD.2004.825125

[17] R. K. Pachar, H. Tiwari, and R. C. Bansal, "A decisive evaluation of parks transformation based commonly used voltage detection method," 2014

[18] B. Tian, C. Mao, J. Lu, D. Wang, Y. He, Y. Duan, et al., "400 V/1000 kVA hybrid automatic transfer switch," IEEE Transactions on Industrial Electronics, vol. 60, pp. 5422-5435, Jan. 2013. doi:10.1109/TIE.2013.2238872

[19] F. R. Zaro, S. O. Al-Takrouri, and M. A. Abido, "Efficient on-line detection scheme of voltage events using quadrature method," Sep. 2018. doi:10.18178/ijeetc.180408

[20] F. Dekhandji, "Signal processing deployment in power quality disturbance detection and classification," Acta Phys Pol, A, vol. 132, pp. 415-419, 2017. doi:10.12693/APhysPolA.132.415

[21] M. B. Latran and A. Teke, "A novel wavelet transform based voltage sag/swell detection algorithm," International Journal of Electrical Power & Energy Systems, vol. 71, pp. 131-139, Oct. 2015. doi:10.1016/j.ijepes.2015.02.040

[22] F. Z. Dekhandji, "Detection of power quality disturbances using discrete wavelet transform," in 2017 5th International Conference on Electrical Engineering-Boumerdes (ICEE-B), 2017, Boumerdes, pp. 1-5. doi:10.1109/ICEE-B.2017.8192080

[23] F. Ucar, O. F. Alcin, B. Dandil, and F. Ata, "Power quality event detection using a fast extreme learning machine," Energies, vol. 11, p. 145, Jan. 2018. doi:10.3390/en11010145

[24] M. Lopez-Ramirez, E. Cabal-Yepez, L. M. Ledesma-Carrillo, H. Miranda-Vidales, C. Rodriguez-Donate, and R. A. Lizarraga-Morales, "FPGA-based online PQD detection and classification through DWT, mathematical morphology and SVD," Energies, vol. 11, p. 769, Mar. 2018. doi:10.3390/en11040769

[25] J. Li, Z. Teng, Q. Tang, and J. Song, "Detection and classification of power quality disturbances using double resolution S-transform and DAG-SVMs," IEEE Transactions on Instrumentation and Measurement, vol. 65, pp. 2302-2312, Jun. 2016. doi:10.1109/TIM.2016.2578518

[26] R. Kapoor, R. Gupta, S. Jha, and R. Kumar, "Boosting performance of power quality event identification with KL divergence measure and standard deviation," Measurement, vol. 126, pp. 134-142, Oct. 2018. doi:10.1016/j.measurement.2018.05.053

[27] A. Shaik and A. S. Reddy, "Flexible entropy based feature selection and multi class SVM for detection and classification of power quality disturbances," International Journal of Intelligent Engineering and Systems, vol. 11, Apr. 2018. doi:10.22266/ijies2018.1031.13

[28] T. Zhong, S. Zhang, G. Cai, Y. Li, B. Yang, and Y. Chen, "Power quality disturbance recognition based on multiresolution s-transform and decision tree," IEEE Access, vol. 7, pp. 88380-88392, Jun. 2019. doi:10.1109/ACCESS.2019.2924918

[29] K. Thirumala, S. Pal, T. Jain, and A. C. Umarikar, "A classification method for multiple power quality disturbances using EWT based adaptive filtering and multiclass SVM," Neurocomputing, vol. 334, pp. 265-274, Mar. 2019. doi:10.1016/j.neucom.2019.01.038

[30] O. Jeba Singh, D. Prince Winston, B. Chitti Babu, S. Kalyani, B. Praveen Kumar, M. Saravanan, et al., "Robust detection of real-time power quality disturbances under noisy condition using FTDD features," Automatika, vol. 60, pp. 11-18, Jan. 2019. doi:10.1080/00051144.2019.1565337

[31] D. De Yong, S. Bhowmik, and F. Magnago, "An effective power quality classifier using wavelet transform and support vector machines," Expert Systems with Applications, vol. 42, pp. 6075-6081, Sep. 2015. doi:10.1016/j.eswa.2015.04.002

[32] M. Lopez-Ramirez, L. Ledesma-Carrillo, E. Cabal-Yepez, C. Rodriguez-Donate, H. Miranda-Vidales, and A. Garcia-Perez, "EMD-based feature extraction for power quality disturbance classification using moments," Energies, vol. 9, p. 565, Jul. 2016. doi:10.3390/en9070565

[33] R. Kumar, B. Singh, and D. T. Shahani, "Recognition of single-stage and multiple power quality events using Hilbert–Huang transform and probabilistic neural network," Electric Power Components and Systems, vol. 43, pp. 607-619, Mar. 2015. doi:10.1080/15325008.2014.999147

[34] M. Gok and I. Sefa, "Research and implementation of a USB interfaced real-time power quality disturbance classification system," Advances in Electrical and Computer Engineering, vol. 17, pp. 61-71, Aug. 2017. doi:10.4316/AECE.2017.03008

[35] M. I. Gursoy, A. S. Yilmaz, and S. V. Ustun, "A practical real-time power quality event monitoring applications using discrete wavelet transform and artificial neural network," Journal of Engineering Science and Technology (JESTEC), vol. 13, pp. 1764-1781, 2018

[36] O. I. Abiodun, A. Jantan, A. E. Omolara, K. V. Dada, A. M. Umar, O. U. Linus, et al., "Comprehensive review of artificial neural network applications to pattern recognition," IEEE Access, vol. 7, pp. 158820-158846, Oct. 2019. doi:10.1109/ACCESS.2019.2945545

[37] A. K. Sadigh and K. Smedley, "Fast and precise voltage sag detection method for dynamic voltage restorer (DVR) application," Electric Power Systems Research, vol. 130, pp. 192-207, Jan. 2016. doi:10.1016/j.epsr.2015.08.002

[38] M. S. Manikandan, S. Samantaray, and I. Kamwa, "Detection and classification of power quality disturbances using sparse signal decomposition on hybrid dictionaries," IEEE Transactions on Instrumentation and Measurement, vol. 64, pp. 27-38, Jun. 2014. doi:10.1109/TIM.2014.2330493

[39] R. Kumar, B. Singh, and D. Shahani, "Symmetrical components-based modified technique for power-quality disturbances detection and classification," IEEE Transactions on Industry Applications, vol. 52, pp. 3443-3450, Mar. 2016. doi:10.1109/TIA.2016.2536665

[40] J. Ma, J. Zhang, L. Xiao, K. Chen, and J. Wu, "Classification of power quality disturbances via deep learning," IETE Technical Review, vol. 34, pp. 408-415, Jul. 2016. doi:10.1080/02564602.2016.1196620

[41] E. A. Nagata, D. D. Ferreira, C. A. Duque, and A. S. Cequeira, "Voltage sag and swell detection and segmentation based on independent component analysis," Electric Power Systems Research, vol. 155, pp. 274-280, Feb. 2018. doi:10.1016/j.epsr.2017.10.029

[42] V. A. Katić and A. M. Stanisavljević, "Smart detection of voltage dips using voltage harmonics footprint," IEEE Transactions on Industry Applications, vol. 54, pp. 5331-5342, Mar. 2018. doi:10.1109/TIA.2018.2819621

[43] V. A. Katić, A. M. Stanisavljević, R. L. Turović, B. P. Dumnić, and B. P. Popadić, "Extended Kalman filter for voltage dips detection in grid with distributed energy resources," in 2018 IEEE PES Innovative Smart Grid Technologies Conference Europe (ISGT-Europe), 2018, Sarajevo, pp. 1-6. doi:10.1109/ISGTEurope.2018.8571857

[44] P. N. Kumawat, D. K. Verma, and N. Zaveri, "Comparison between wavelet packet transform and M-band wavelet packet transform for identification of power quality disturbances," Power Research, vol. 14, pp. 37-45, Jun. 2018. doi:10.33686/pwj.v14i1.142183

[45] W. Qiu, Q. Tang, J. Liu, Z. Teng, and W. Yao, "Power quality disturbances recognition using modified s transform and parallel stack sparse auto-encoder," Electric Power Systems Research, vol. 174, p. 105876, Sep. 2019. doi:10.1016/j.epsr.2019.105876

[46] H. Wang, J. Liu, S. Luo, and X. Xu, "Research on power quality disturbance detection method based on improved ensemble empirical mode decomposition," Electronics, vol. 9, p. 585, Mar. 2020. doi:10.3390/electronics9040585

[47] E. G. Ribeiro, T. M. Mendes, G. L. Dias, E. R. Faria, F. M. Viana, B. H. Barbosa, et al., "Real-time system for automatic detection and classification of single and multiple power quality disturbances," Measurement, vol. 128, pp. 276-283, Nov. 2018. doi:10.1016/j.measurement.2018.06.059

[48] S. Jamali, A. R. Farsa, and N. Ghaffarzadeh, "Identification of optimal features for fast and accurate classification of power quality disturbances," Measurement, vol. 116, pp. 565-574, Feb. 2018. doi:10.1016/j.measurement.2017.10.034

[49] U. Singh and S. N. Singh, "A new optimal feature selection scheme for classification of power quality disturbances based on ant colony framework," Applied Soft Computing, vol. 74, pp. 216-225, Jan. 2019. doi:10.1016/j.asoc.2018.10.017

[50] H. Erişti, A. Uçar, and Y. Demir, "Wavelet-based feature extraction and selection for classification of power system disturbances using support vector machines," Electric power systems research, vol. 80, pp. 743-752, Jul. 2010. doi:10.1016/j.epsr.2009.09.021

[51] F. A. Borges, R. A. Fernandes, I. N. Silva, and C. B. Silva, "Feature extraction and power quality disturbances classification using smart meters signals," IEEE Transactions on Industrial Informatics, vol. 12, pp. 824-833, Oct. 2015. doi:10.1109/TII.2015.2486379

[52] H. Erişti and Y. Demir, "An efficient feature extraction method for classification of power quality disturbances," in Int. Conf. on Power Systems Transients (IPST2009), in Kyoto, Japan, 2009

[53] S. Aziz, M. Awais, T. Akram, U. Khan, M. Alhussein, and K. Aurangzeb, "Automatic scene recognition through acoustic classification for behavioral robotics," Electronics, vol. 8, p. 483, Apr. 2019. doi:10.3390/electronics8050483

[54] S. Aziz, M. U. Khan, Z. A. Choudhry, A. Aymin, and A. Usman, "ECG-based biometric authentication using empirical mode decomposition and support vector machines," in 2019 IEEE 10th Annual Information Technology, Electronics and Mobile Communication Conference (IEMCON), 2019, Vancouver, pp. 0906-0912. doi:10.1109/IEMCON.2019.8936174

[55] M. U. Khan, S. Aziz, S. Ibraheem, A. Butt, and H. Shahid, "Characterization of term and preterm deliveries using electrohysterograms signatures," in 2019 IEEE 10th Annual Information Technology, Electronics and Mobile Communication Conference (IEMCON), 2019, Vancouver, pp. 0899-0905. doi:10.1109/IEMCON.2019.8936292

[56] M. U. Khan, S. Aziz, K. Iqtidar, A. Zainab, and A. Saud, "Prediction of acute coronary syndrome using pulse plethysmograph," in 2019 4th International Conference on Emerging Trends in Engineering, Sciences and Technology (ICEEST), 2019, Karachi, pp. 1-6. doi:10.1109/ICEEST48626.2019.8981690

[57] M. U. Khan, S. Aziz, A. Malik, and M. A. Imtiaz, "Detection of myocardial infarction using pulse plethysmograph signals," in 2019 International Conference on Frontiers of Information Technology (FIT), 2019, Islamabad, pp. 95-955. doi:10.1109/FIT47737.2019.00027

[58] T. Andrews, "Computation time comparison between Matlab and C++ using launch windows," 2012.

[59] H. Yu and B. M. Wilamowski, "C++ implementation of neural networks trainer," in 2009 International Conference on Intelligent Engineering Systems, 2009, Barbados, pp. 257-262. doi:10.1109/INES.2009.4924772

[60] W. L. Rodrigues Junior, F. A. Borges, R. d. A. Rabelo, J. J. Rodrigues, R. A. Fernandes, and I. N. da Silva, "A methodology for detection and classification of power quality disturbances using a real-time operating system in the context of home energy management systems," International Journal of Energy Research, 2020

[61] M. R. Al Koutayni, V. Rybalkin, J. Malik, A. Elhayek, C. Weis, G. Reis, et al., "Real-time energy efficient hand pose estimation: A Case Study," Sensors, vol. 20, p. 2828, May 2020. doi:10.3390/s20102828

[62] M. Mishra, "Power quality disturbance detection and classification using signal processing and soft computing techniques: A comprehensive review," International Transactions on Electrical Energy Systems, vol. 29, p. e12008, Mar. 2019. doi:10.1002/2050-7038.12008

[63] M. U. Khan, S. Aziz, M. Bilal, and M. B. Aamir, "Classification of EMG signals for assessment of neuromuscular disorder using empirical mode decomposition and logistic regression," in 2019 International Conference on Applied and Engineering Mathematics (ICAEM), 2019, Islamabad, pp. 237-243. doi:10.1109/INMIC48123.2019.9022741